

# Propulsion of droplets on micro- and sub-micron ratchet surfaces in the Leidenfrost temperature regime

Jeong Tae Ok · Eugene Lopez-Oña ·  
Dimitris E. Nikitopoulos · Harris Wong ·  
Sungook Park

Received: 30 August 2010 / Accepted: 30 October 2010 / Published online: 21 November 2010  
© Springer-Verlag 2010

**Abstract** Spatially periodic systems with localized asymmetric surface structures (ratchets) can induce directed transport of matter (liquid/particles) in the absence of net force. Here, we show that propulsion for the directed motion of water droplets levitating on heated ratchet surfaces in the Leidenfrost (film boiling) regime is significantly enhanced as the ratchet period decreases down to micro- and sub-micrometers. At the temperature range slightly above the threshold temperature of droplet motion, sub-micron ratchets yield water droplet velocities reaching  $\sim 40$  cm/s, a speed that has never been achieved with any chemical and topological gradient surfaces. This dramatic increase in the droplet velocity is attributed to an enhanced heat transfer through the local contacts between ratchet peaks and bottom of the droplet. A hydrophobic coating on the ratchet surfaces is found to further increase the droplet velocity and decrease the threshold temperature of the droplet motion. The results suggest that miniaturized ratchet surfaces can potentially be used in diverse applications requiring control over fluid transport and heat transfer such as two phase cooling systems for microprocessors and fuel injection for combustion technology and that for those applications the design of ratchet dimensions and surface chemistry are critically important.

**Keywords** Micro- and nanoscale ratchets · Leidenfrost (film-boiling) phenomenon · Droplet motion · Heat transfer

## List of symbols

$d$	Depth of ratchet, $\mu\text{m}$
$D_0$	Initial diameter of droplet, mm
DI	Deionized
$g$	Gravity, $\text{m/s}^2$
$h$	Height of step for ratchet fabrication, $\mu\text{m}$
$h_v$	Vapor layer thickness above ratchet peaks
H	Higher temperature
$H_p$	Height of pipette tip for dispensing droplets, mm
$l$	Length of step for ratchet fabrication, $\mu\text{m}$
Ni	Nickel
L	Lower temperature
$p$	Period of ratchet, $\mu\text{m}$
$R$	Radius of droplet, mm
$T_b$	Boiling temperature, $^\circ\text{C}$
$T_{\text{Th}}$	Threshold temperature for rectified droplet motion, $^\circ\text{C}$
$T_L$	Leidenfrost temperature, $^\circ\text{C}$
$\Delta T$	Surface temperature with respect to the boiling temperature of the liquid, $^\circ\text{C}$
$v_0$	Initial impact velocity of droplets on ratchet surfaces, m/s
$V_0$	Initial volume of droplet, $\mu\text{l}$
$v_{\text{max}}$	maximum mean velocity, cm/s
$We$	Weber number
$\Delta z$	Maximum vertical variation for the sample surface, $\mu\text{m}$

J. T. Ok · E. Lopez-Oña · D. E. Nikitopoulos · H. Wong ·  
S. Park (✉)  
Mechanical Engineering Department, Louisiana State  
University, 2508 Patrick F. Taylor Hall, Baton Rouge,  
LA 70803, USA  
e-mail: sungook@me.lsu.edu

J. T. Ok · D. E. Nikitopoulos · S. Park  
Center for Bio-Modular Multiscale Systems, Louisiana State  
University, 2508 Patrick F. Taylor Hall, Baton Rouge,  
LA 70803, USA

## Greek symbols

$\rho$	Density, $\text{kg/m}^3$
$\gamma$	Surface tension, N/m

## 1 Introduction

Motion of matter requires application of asymmetric potential. Fluids are conventionally driven by applying macroscopic net asymmetric potentials such as pressure gradient by a pump or compressor, and electric field between two electrodes. Net asymmetric potentials produced by an imbalance of surface tension forces (Marangoni effect) via a chemical (Chaudhury and Whitesides 1992; Brochard 1989; Dos Santos et al. 1995; John et al. 2005; Daniel et al. 2001), thermal (Brochard 1989; Brzoska et al. 1993; Darhuber et al. 2003), or electrical gradient (Thiele et al. 2004) were also used. However, these methods either require an external power source for driving a motion or have a limitation in the displacement due to a finite length of the gradient that can be produced. On the other hand, spatially periodic systems with localized asymmetric structures (ratchets) can induce directed transport of liquid/particles in the absence of net force, and thus have recently received much attention as a means of rectifying motion for many applications.

Ratchets have been used for quantum tunneling ratchets (Linke et al. 1999, 2002), dielectrophoretic rectification of Brownian motion (Hughes 2004) and action of molecular motors (Kulic et al. 2005; Julicher et al. 1997). Topological ratchet structures were also used as a rectifier that forces the otherwise random mechanical motion of droplets into a specific direction by means of localized asymmetric potential (Linke et al. 2006; Buguin et al. 2002; Ding et al. 2007, 2009). To induce motion, topological ratchet structures that rectify the direction of motion need to be combined with a fluctuation to overcome the pinning of the droplet to the surface. Buguin et al. (2002) triggered fluctuation in the shape of droplet and wetting properties by various physical ways either with an on/off electric field, or with a low frequency electric field of zero mean value, or by mechanically vibrating the substrate with a standard audio speaker. The velocities along the ratchets were observed up to a few mm/s. Ding et al. (2009) utilized lateral vibration through a sinusoidal shaker with a controllable frequency and amplitude in order to move droplets within microchannels whose sidewalls were decorated with topological ratchets produced by photolithography. Droplet velocity depends on vibration parameters such as amplitude and frequency as well as on channel parameters such as geometry, material, and the lateral offset angle. A maximum droplet velocity of 10 cm/s was observed with a vibration frequency 50 Hz and lateral amplitude 3.5 mm from silicon channel. Another way to achieve such a fluctuation of droplet height has been demonstrated by Linke et al. (2006), where millimeter scale saw-tooth surface profiles machined into brass were heated to the Leidenfrost regime (the film-boiling regime). In the

Leidenfrost regime, liquid evaporates at the bottom surface of the droplet due to heating of a substrate and a thin vapor layer is formed between liquid droplets and a heated surface, which reduces the heat transfer and thus retards the evaporation. The Leidenfrost temperature ( $T_L$ ) is defined as a temperature in the boiling regime where the lifetime of droplets is the longest. In the presence of topological ratchet structures, the pressure that levitates the droplet pushes out the vapor laterally and the ratchet surface partially rectifies this vapor flow, exerting a net viscous force on the droplet (Linke et al. 2006). With the millimeter scale ratchets, the droplet velocity of a few cm/s was achieved. Despite the demonstration of using ratchets to rectify motion of droplets, however, there have been no efforts to extend this driving mechanism to micro- and nanoscale ratchets, which is a critical step toward micro- and nanofluidic applications.

In this article, we systematically examine this driving mechanism with ratchets of millimeter down to sub-micrometer period. Ratchets with various periods were produced into either brass or nickel via micromachining techniques and the velocity of droplets on the heated ratchet surfaces in the Leidenfrost regime was measured. We found that the propulsion of droplet motion is significantly enhanced as the ratchet period becomes smaller, which is attributed to an enhanced heat transfer between the bottom of the droplet and the surface ratchets. We also studied the influence of surface wettability on the droplet motion.

## 2 Experimental

### 2.1 Micro and sub-micron ratchet fabrication

Two different types of ratchets were fabricated: (1) brass ratchets with periods from millimeter down to 15  $\mu\text{m}$  directly milled by a micromilling machine and (2) sub-micron period nickel (Ni) ratchets replicated by electroplating from a polymer optical grating. Figure 1 shows the fabrication step of brass ratchets which consists of three steps: tapered milling, step micromilling, and backside planarization. Brass was selected as the ratchet material due to its large thermal conductivity required for the film-boiling droplet experiments as well as its excellent machinability for micromilling. First, a brass bar ( $5 \times 2 \times 1 \text{ inch}^3$ , Alloy 353, McMaster-Carr, Atlanta, GA) was milled using a CNC milling machine (CNC Hass VF-2YT, CA) to have a tapered angle that was determined by the aspect ratio of designed ratchets to fabricate. A tapered angle was 11.3° in order to achieve aspect ratio of 0.2. This step is needed to reduce process time for the subsequent micromilling process. The second step is to

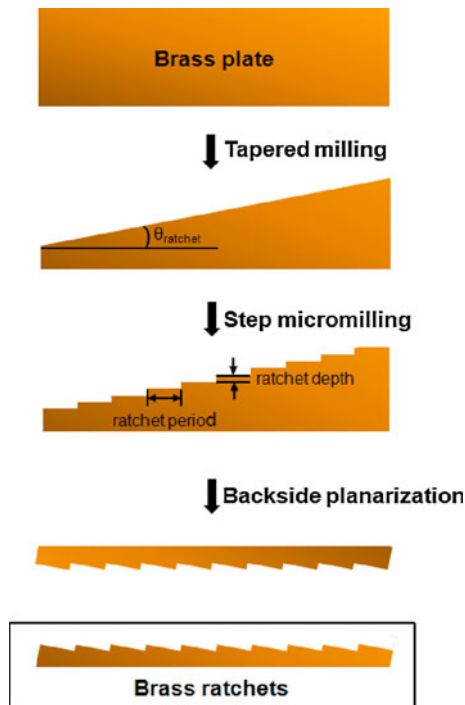


**Fig. 1** Process scheme for the fabrication of miniaturized ratchets in brass by micromilling

produce micro- to millimeter scale steps in the CNC-milled, tapered brass bar using a micro milling machine (KERN MMP2522, KERN Micro- und Feinwerktechnik GmbH & Co. KG, Germany). The micro milling bit (radius 100–1500  $\mu\text{m}$ ) was carried on a spindle at a maximum rpm of 40,000 and the resolution of position and repetition was  $\pm 1 \mu\text{m}$ . The spindle speed used for micro milling was 3,500 rpm. The root mean square roughness for the surfaces produced by the micro milling technique was typically  $\sim 300 \text{ nm}$  (Kim et al. 2008). As the last step, backside planarization was done with the conventional milling process, while protecting the micro-milled step surface with a piece of thick (1/2 inch) silicone rubber sheet (NSF-certified silicone rubber sheet, McMaster-Carr, Atlanta, GA). The areas of the brass-ratcheted surfaces fabricated were  $5 \times 10 \text{ cm}^2$ , while the replicated Ni ratchets have the patterned area of  $5.2 \times 5.2 \text{ cm}^2$ . All the fabricated ratchets were inspected using profilometer, optical microscope, scanning electron microscope (SEM), and atomic force microscope (AFM) prior to use for droplet motion experiments.

## 2.2 Droplet motion experiments

Figure 2 shows the experimental setup used to investigate droplet motion on heated ratchet surfaces. It consists of three parts: a hot plate for heating ratchet samples, a micropipette for injection of droplets, and a video camera

for recording the droplet motion. The micro-manufactured brass or Ni ratchets were placed on a digital ceramic hot plate (Isotemp, Fisher Scientific). After reaching a constant temperature from the display in the hot plate, we waited for an hour to reach a thermal equilibrium and then measured ratchet surface temperatures at four corners and the center with a K-type thermocouple (TP 873/TP 882, EXTECH) and thermometer (ML720, EXTECH). The accuracy of temperature measurements with the thermocouple and thermometer was  $\pm 0.3\%$  according to the specification provided by the manufacturer. The averaged temperature was used as ratchet surface temperature. Usually the difference for temperatures measured at the four corners is in the range of 0–15°C. Then, droplets of constant volume were dispensed using a commercial micropipette (Eppendorf) with the volume ( $V_0$ ) in the range of 3–6  $\mu\text{l}$  with a delay of 4–5 s imposed between the releases of successive droplets. In this range of volume, the droplet diameter is smaller than the capillary length of water which is 2.5 mm at 100°C. Thus, the shape of droplets is close to a sphere except for the bottom surface which may be deformed along the ratcheted topology. In spite of manual dispense, the height of the pipette tip ( $H_p$ ) was controlled to be in the range of 2–5 mm from the ratchet surface, which corresponds to Weber numbers of 0–1.9 for the droplet volume of 5  $\mu\text{l}$ . The Weber number is defined as  $(We = \frac{\rho D_0 v_0^2}{\gamma})$ , where  $\rho$  and  $\gamma$  are the density and surface tension of water droplet at its boiling temperature ( $\rho = 960 \text{ kg/m}^3$  and  $\gamma = 59 \text{ mN/m}$  at  $T_b = 100^\circ\text{C}$ ). The impact velocity was determined by the released height  $H_p$  and initial droplet diameter  $D_0$  using the equation  $v_0 = \sqrt{2g(H_p - D_0)}$ , where  $g$  is gravity, which gives the impact velocities of 0–0.26 m/s. The Weber number is a dimensionless number showing relative importance of the kinetic energy of a fluid to its surface tension. Thus, a low Weber number in a similar range implies that initial impact of droplet on the ratcheted surface will contribute to the mean velocity in a similar way for all experiments and thus comparison of mean velocities for different samples is meaningful.

Droplet trajectory was captured using a video camera (Sony DSC-V1, 16 frames per second) and the Windows Movie Maker (Microsoft) software was used for tracking and processing the captured videos. Since the acceleration

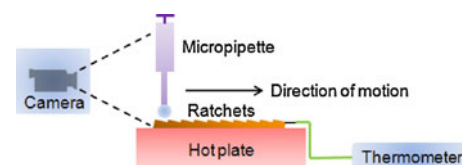


**Fig. 2** Schematic diagram of the experimental setup to investigate motion of Leidenfrost droplets on ratchets

of the droplet could not be properly monitored with the video camera used due to its resolution limit and an equilibrium velocity was not reached within the length of the fabricated ratchets, we simply took the mean velocity for data analysis, which was obtained by the distance travelled by the droplet before it escaped from the ratchet surface divided by time. At least the motion of 10 droplets was captured for each ratchet surface temperature and the velocity values were averaged to obtain a single data point.

### 2.3 Fluorinated silane coating on ratchet surfaces

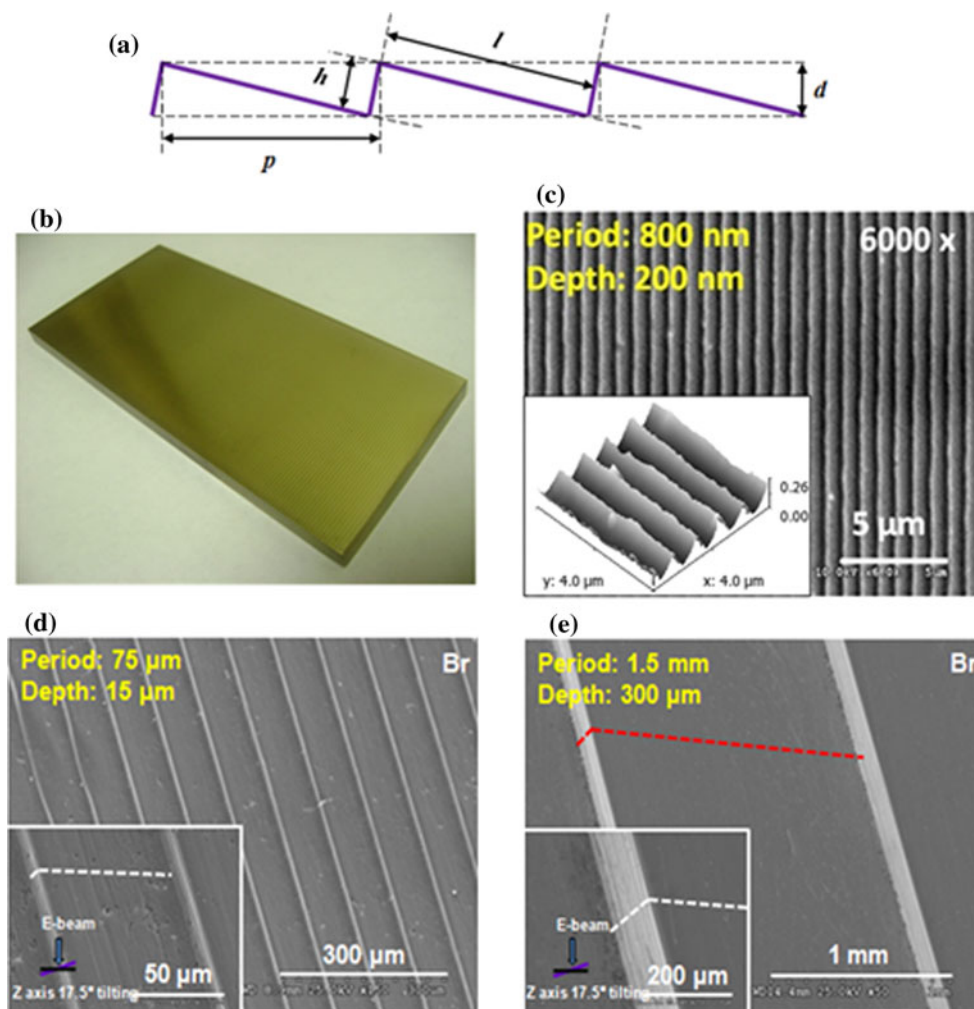
In order to investigate the effect of the surface wettability on the droplet motion, the ratchet surfaces were coated with a hydrophobic fluorinated silane, 1H,1H,2H,2H-perfluorodecyltrichlorosilane. Prior to the coating, the ratchet surface was exposed to O<sub>2</sub> plasma for 3 min with 150 W, 75 mTorr. The coating with a hydrophobic fluorinated silane was performed for 10 min in the vapor phase in a custom-designed chemical vapor deposition chamber.

## 3 Results and discussion

### 3.1 Micro- and sub-micron ratchet fabrication

One critical requirement for the fabrication of ratchets is that the ratcheted surface area has to be large enough to enable observation of the development of rectified droplet motion in a direction after initial impact on the surface. In addition, since we are interested in studying the effect of the ratchet period, the ratchet aspect ratio, defined as the ratio of depth-to-period, needs to be kept similar to each other. Even though it is expected that all ratchet parameters will have effects on the droplet motion separately, this work is limited to the study of ratchets with one aspect ratio, mostly because it is time-consuming to produce large area ratchet samples. Figure 3a shows definitions of ratchet dimensions used in this study. Since it is miniaturized steps, not ratchets, that were directly milled by the micromilling process, two different sets of period and depth are defined in the fabrication of a ratchet surface:  $l$  and

**Fig. 3** **a** Definition of period and depth of miniaturized ratchets and steps, **b** a photograph of large area brass ratchets with 750  $\mu\text{m}$  period produced by micromilling, **c–e** scanning electron micrographs and atomic force microscopy image of various miniaturized ratchets



$h$  represent the period and step height for miniaturized steps in the micromilling process, while  $p$  and  $d$  are the period and depth for the final ratchets after backside planarization. For convenience, we will use the designed step period to indicate the period of a ratchet in this article, since the deviation between the two is small.

Figure 3b shows an example photograph of a large area brass ratchet sample with 750  $\mu\text{m}$  period after completing the entire milling procedures described in Fig. 1. The size of the ratchets is  $5 \times 2 \times 1/4 \text{ inch}^3$  and the measured period and depth of the ratchets were  $768.1 \pm 3.0 \mu\text{m}$  period and  $127.6 \pm 2.6 \mu\text{m}$ , respectively. Figure 3c–e shows example micrographs of miniaturized ratchets with different dimensions: nickel ratchets with 800 nm period and brass ratchets with 75 and 1500  $\mu\text{m}$  periods. For all samples, saw-tooth like asymmetric topological structures are clearly visible. The dimensions of fabricated ratchets were obtained using surface profiles measured with a stylus profilometer and atomic force microscope for respective microscale and submicron ratchets, which are summarized in Table 1. Each value in the table was obtained by averaging from at least three different measurements. Four different ratchets with designed step periods of 15, 75, 150, and 1500  $\mu\text{m}$  were fabricated via micromilling, which leads to actual ratchet periods of  $15.3 \pm 0.2$ ,  $76.7 \pm 1.1$ ,  $150.4 \pm 1.8$  and  $1499 \pm 15.7 \mu\text{m}$  after fabrication. The root mean square roughness for the surfaces produced by the micromilling technique was typically  $\sim 300 \text{ nm}$  (Kim et al. 2008).

It is important to keep the aspect ratio in a similar range in order to investigate the effect of ratchet period. The designed aspect ratio for microratchets was 0.2 (1:5). After fabrication, the measured aspect ratio values also deviated slightly from the designed values, showing 0.25, 0.16, 0.16, 0.16 and 0.15 for the ratchet periods of 0.8, 15, 75, 150, and 1500  $\mu\text{m}$ , respectively. But they were still in the similar range of 0.2. Maximum vertical variations for the sample surfaces ( $\Delta z$ ) generated by series of milling process including backside planarization, was low, in the range of

40–220  $\mu\text{m}$  over 8 cm scan length. Thus, the influence of the surface slope on the droplet motion can be neglected.

### 3.2 Effect of ratchet periods on droplet velocity

Motion of water droplets dispensed on the ratchets with different periods was investigated while the ratchets were heated on a hot plate. The volume of the de-ionized (DI) water droplet used was 5  $\mu\text{l}$ . At ratchet surface temperature below the boiling point of water, droplets put on ratchet surfaces immediately spread and form a certain contact angle at the three phase interface depending on the temperature. When the temperature exceeds the boiling point, droplets start to boil vehemently via nucleation boiling and disappear rapidly due to evaporation. As the ratchet surface temperature increases further and reaches a certain temperature, rectified motion of droplets starts to occur, with no noticeable change in the droplet volume until the droplet escapes from the ratcheted surface. We define this temperature as threshold temperature ( $T_{\text{Th}}$ ) for droplet motion for a specific ratchet surface and, practically,  $T_{\text{Th}}$  was taken as the temperature which clearly shows unidirectional motion of droplets.  $T_{\text{Th}}$  is close to the Leidenfrost temperature ( $T_{\text{L}}$ ) of water. However, the two temperatures ( $T_{\text{Th}}$  and  $T_{\text{L}}$ ) are not the same, as will be discussed later. In the Leidenfrost regime, a liquid droplet on a hot surface produces an insulating vapor layer around it, being separated from the surface. The vapor layer keeps the droplet from boiling rapidly. For water,  $T_{\text{L}}$  was reported to be in the range of 155–515°C, depending on types of surface, surface cleanness and roughness (Bernardin and Mudawar 1999). In the presence of surface ratchets, asymmetric potential for unidirectional motion is given by a saw-tooth-shaped surface topology, while the vapor layer provides fluctuating force vertical to the ratchet surface to help overcome pinning of the droplet to the surface. The motion was observed perpendicular to the ratcheted grooves and in the direction toward the slowly inclined side from ratchet peaks, which is in agreement with the direction of droplet

**Table 1** Designed and fabricated dimensions of miniaturized ratchets used in this study

Sample name	Designed					Measured					
	$l$ ( $\mu\text{m}$ )	$h$ ( $\mu\text{m}$ )	$p$ ( $\mu\text{m}$ )	$d$ ( $\mu\text{m}$ )	$d/p$	$l$ ( $\mu\text{m}$ )	$h$ ( $\mu\text{m}$ )	$p$ ( $\mu\text{m}$ )	$d$ ( $\mu\text{m}$ )	$d/p$	$\Delta z$ ( $\mu\text{m}$ )
800 nm	–	–	0.8	0.2	0.25	–	–	0.8	0.2	0.25	$\sim 85$
15 $\mu\text{m}$	15	3	15.3	2.9	0.19	$15.3 \pm 0.4$	$2.7 \pm 0.1$	$15.3 \pm 0.2$	$2.4 \pm 0.2$	0.16	$\sim 60$
75 $\mu\text{m}$	75	15	76.5	14.7	0.19	$75.4 \pm 0.0$	$12.9 \pm 0.2$	$76.7 \pm 1.1$	$12.0 \pm 0.1$	0.16	$\sim 50$
150 $\mu\text{m}$	150	30	153	29.4	0.19	$146.0 \pm 0.6$	$27.7 \pm 0.1$	$150.4 \pm 1.8$	$24.3 \pm 1.6$	0.16	$\sim 220$
1.5 mm	1500	300	1529.7	294.2	0.19	$1486 \pm 13.1$	$281.5 \pm 8.1$	$1499 \pm 15.7$	$230.5 \pm 2.3$	0.15	$\sim 40$

$\Delta z$  is maximum vertical variation over the scan length. The scan lengths were 4 cm for sub-micron ratchets with 800 nm period and 8 cm for all other micromilled brass samples

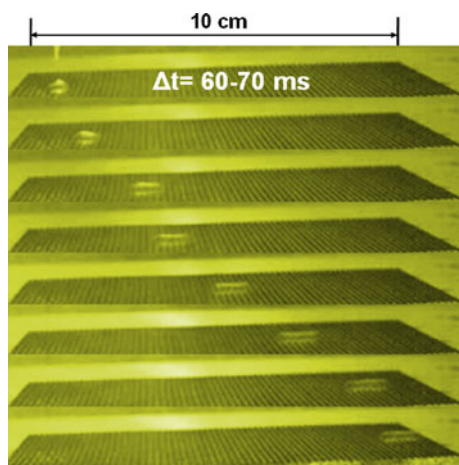


**Fig. 4** A sequence of video images for droplet motion on 1.5 mm period ratchets. The droplet moves perpendicular to ratchet grooves along the slowly inclined side from ratchet peaks

motion observed by Linke et al. (2006). Figure 4 presents a sequence of video images showing an example of droplet motion of de-ionized water on brass ratchets with 1500  $\mu\text{m}$  period and 230  $\mu\text{m}$  depth at a surface temperature of 254°C.

Figure 5a shows the mean droplet velocity as a function of surface temperature for different ratchet periods. As the surface temperature increases beyond  $T_{\text{Th}}$  for droplet motion, the velocity first increases rapidly and reaches a maximum, and then decreases. Two temperature regimes can be identified. At temperatures just above  $T_{\text{Th}}$  (L regime), a dramatic increase in the droplet velocity was observed with decreasing ratchet period. It even reached over 40 cm/s for 0.8  $\mu\text{m}$  ratchet period. Considering that the velocity used in this study was obtained by taking a mean value from the beginning of droplet motion to droplet escape from the ratcheted surface, not an equilibrium velocity, the instantaneous velocity at the droplet escape would be larger than the average velocity. To our knowledge such propulsion is unprecedented with any droplet motion achieved by a surface tension gradient and topological ratchets without an external device such as syringe pumps and electrodes. The droplet velocity achieved with such surfaces with a surface tension gradient and topological ratchets was in the range from a few mm/s (Chaudhury and Whitesides 1992; Daniel et al. 2001; Buguin et al. 2002) to a few cm/s (Dos Santos et al. 1995; Linke et al. 2006). In the second temperature regime much higher than  $T_{\text{Th}}$  (H regime), the droplet velocity slightly decreases with increasing temperature around values of a few cm/s without dependence on the ratchet period. These two regimes were also observed for other liquids including acetone ( $T_{\text{L}} = 132^\circ\text{C}$ ) and R134a ( $T_{\text{L}} = 20^\circ\text{C}$ ).

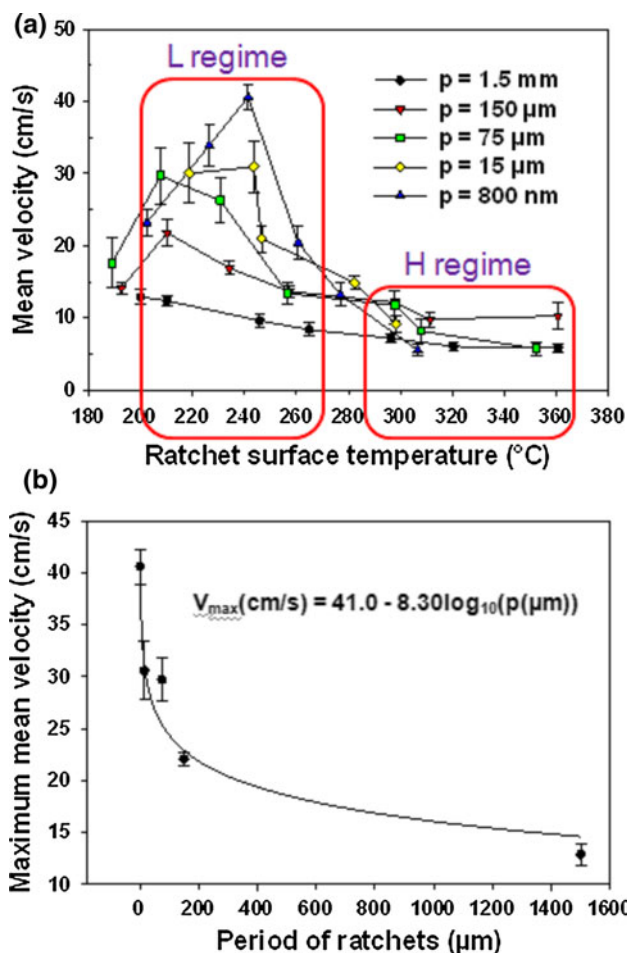


**Fig. 5** **a** Mean droplet velocity as a function of ratchet surface temperature for ratchets with different periods. At temperatures just above  $T_{\text{Th}}$  (L regime), the mean droplet velocity significantly increases with decreasing ratchet period, while in the higher temperature regime the velocity remains constant at a few cm/s, and **b** maximum mean droplet velocity as a function of ratchet period. A best logarithmic fit is also included

The strong dependence of ratchet period observed in the first temperature regime can be understood by assuming that the droplet is still in contact with top edges of the ratchets, which is different from the Leidenfrost droplet case where the droplet is fully separated from the surface by a thin vapor layer and the heat transfer between the droplet and ratchets are reduced by the presence of the vapor layer. This is justified because the vapor layer in this temperature regime would be relatively thin. According to a 2-D model for Leidenfrost droplets, the vapor layer thickness is proportional to  $(\Delta T)^{1/3}$ , where  $\Delta T$  is denoted as the temperature with respect to the boiling temperature of the liquid (Biance et al. 2003). The measured value of the vapor layer thickness is typically 10–100  $\mu\text{m}$  on flat surfaces (Biance et al. 2003; Linke et al. 2006). Due to the enhanced heat transfer through the direct local contacts between the ratchet top peaks and the liquid drop, the

liquid drop evaporates mainly right above the peaks of the ratchets. The evaporated vapor is then split by the peak, flows down the two sides into the trenches, and then escapes along the trenches. The vapor on the less inclined side exerts more shear stress on the droplet bottom than that at the steeply inclined side (Linke et al. 2006). Therefore, a single ratchet generates a net driving force on the droplet and the total driving force will depend on the number of ratchets beneath the droplet. This explanation is corroborated with the behavior of droplet motion on ratchet surface with different surface energies, which will be discussed later.

The lifetime of a droplet on a heated surface is longest when the insulating vapor layer entirely covers the droplet bottom. The droplet lifetime on ratchet surfaces could not be measured due to the droplet motion. However, it can be deduced from the presence of direct contacts between ratchet peaks and droplet bottom that droplet motion on the miniaturized ratchet surfaces occurs before  $T_L$  is reached. Thus,  $T_{Th} < T_L$ . The enhanced heat transfer through the ratchet peaks may also enhance thermocapillary flow along the bottom surface of the droplet, which will reduce shear stress at the droplet/vapor interface. However, the thermocapillary effect is expected to be much less pronounced for smaller ratchet periods because the temperature gradient along the bottom surface of the droplet also decreases.

According to theoretical studies (Bernardin and Mudawar 1999; Bernardin and Mudawar 2002; Prat et al. 1995), the presence of surface roughness significantly affects the flow field of vapor underneath a fully levitating droplet mainly in three ways: first, the vapor flow penetrates into the roughness cavities and recirculation develops at the bottom of each cavity; second, as the size of the droplet relative to the size of the roughness increases or as the size of the roughness decreases, while keeping the droplet volume constant, the thickness of the vapor layer above the roughness increases; and third,  $T_L$  increases. In H regime where the dependence of ratchet period on the mean velocity disappeared, the droplet can be considered fully levitating from the surface due to a relatively thick vapor layer. Thus, the heat transfer is expected to be more homogenous over the droplet bottom surface. There can still be local fluctuation in heat transfer along the ratcheted surface topology if the vapor layer thickness above the ratchet peaks is not sufficiently large compared to the ratchet depth. However, even in this case, as the ratchet period decreases, the positive effect from the increased number of ratchets on droplet propulsion will be cancelled by the negative effect of increasing vapor layer thickness. Our discussion remained qualitative due to the difficulty in directly measuring the vapor layer thickness underneath droplets. A quantitative description relating the droplet motion to ratchet dimensions and vapor layer thickness

may be possible through modeling this phenomenon by balancing the drag force and the Stoke's drag from the air on the droplet.

Figure 5b plots the maximum mean velocity that is found in the L temperature regime as a function of ratchet period. The maximum mean velocity fits well to the logarithm of ratchet period,  $v_{max}(cm/s) = 41.0 - 8.30 \log_{10}(p(\mu m))$ . The contribution of each ratchet to the droplet motion was estimated by simply normalizing the maximum mean velocity by the effective number of ratchets underneath a droplet, which is shown in Fig. 6. While in our explanation every single ratchet is supposed to generate a net driving force, the contribution of a single ratchet may not be same for different ratchet periods. The contribution of each ratchet to the overall droplet motion decreases linearly with decreasing the ratchet period from millimeter to sub-micron scales. Two different explanations on this behavior are possible. The first explanation involves the vapor layer thickness which increases with decreasing size of surface roughness for a constant droplet volume (Prat et al. 1995). Thus, with smaller ratchets the actual contact area for heat transfer between ratchet peaks and droplet bottom would be smaller due to increased vapor layer thickness, leading to a reduced heat transfer through each ratchet. The other possible explanation is an increased resistance (or friction) against vapor flow with smaller ratchets, which occurs while the vapor escapes from the bottom of the droplet along the ratchet trenches. This is because the area for the triangle formed between the ratchet trenches and the droplet bottom surface through which the vapor escapes decreases with decreased ratchet period, resulting in an increase in friction (Ornatskii 1965). The schematics describing the droplet/vapor layer/ratchet interfaces for two different temperature regimes as well as different ratchet periods are shown in Fig. 7. Nevertheless, the significant increase in the overall droplet mean velocity with decreasing ratchet period suggests that a decrease in the ratchet period to the real nanoscale (sub-100 nm) may further increase propulsion of the droplet motion until the droplet sees the ratchets as a flat surface. Thus, it will be an interesting research topic to investigate the minimum ratchet period that still shows the propulsion of liquid droplets, which may depend on the aspect ratio, surface roughness, and wetting behavior of the ratchets as well as the types of droplets. However, production of large area, nanoscale ratchets with defined geometries is still a great challenge and needs to be developed.

### 3.3 Effect of droplet volume

The influence of droplet volume on the motion of Leidenfrost droplets was investigated with microscale

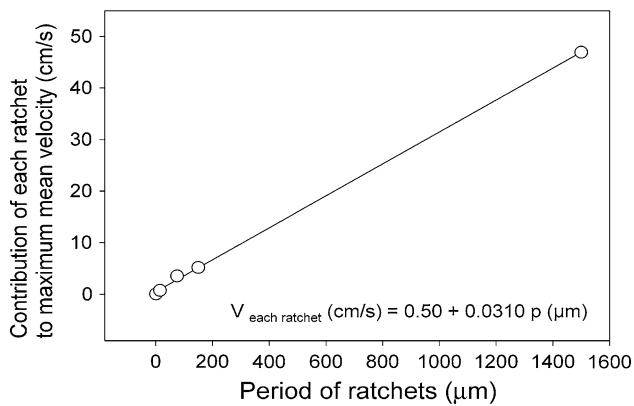


**Fig. 6** Maximum mean velocity normalized by the effective number of ratchets underneath a droplet as a function of ratchet period, which indicates contribution of each ratchet to maximum mean velocity

ratchet samples. According to the observation on Leidenfrost droplets on a flat surface, the shape of droplets and the vapor layer thickness are dependent on the size of droplets (Biance et al. 2003; Linke et al. 2006). Droplet volumes in the range of 3–6  $\mu\text{l}$ , could be manipulated with the micropipette used, which correspond to droplet radii  $R$  of 0.89–1.13 mm, still smaller than the capillary length of water of 2.5 mm at 100°C. When the droplet radius is smaller than the capillary length, the lateral shape of the droplet is almost spherical except at the bottom because surface tension of the droplet governs (Biance et al. 2003). Then, evaporation occurs through the entire droplet surface and the vapor layer thickness was reported to increase

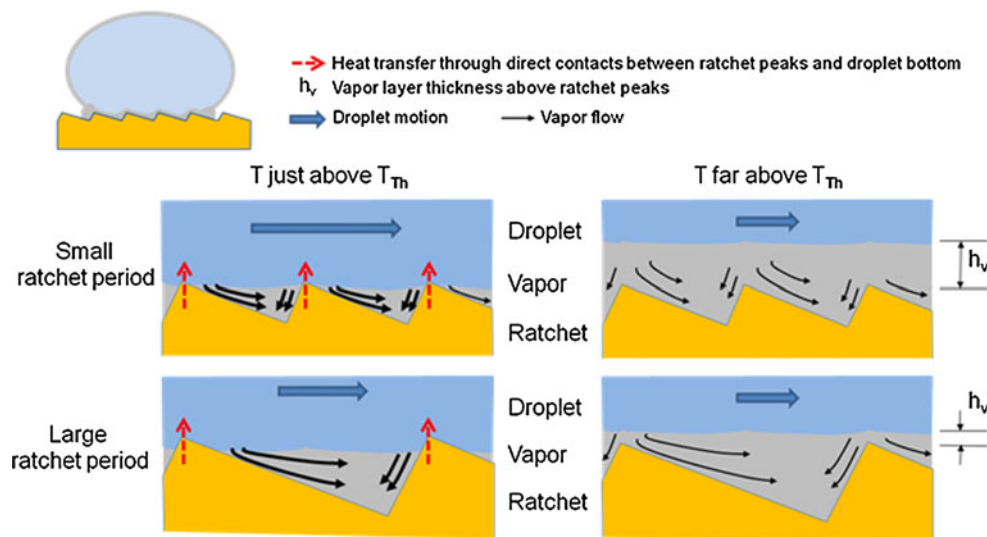


**Fig. 7** Schematics describing the droplet/vapor layer/ratchet interfaces for two different temperature regimes as well as different ratchet periods. At temperatures just above  $T_{Th}$ , there are local contacts between the bottom of the droplet and the peaks of the ratchets, which enhance the heat transfer through the contacts. As a result, the total driving force depends on the number of ratchets beneath the droplet.

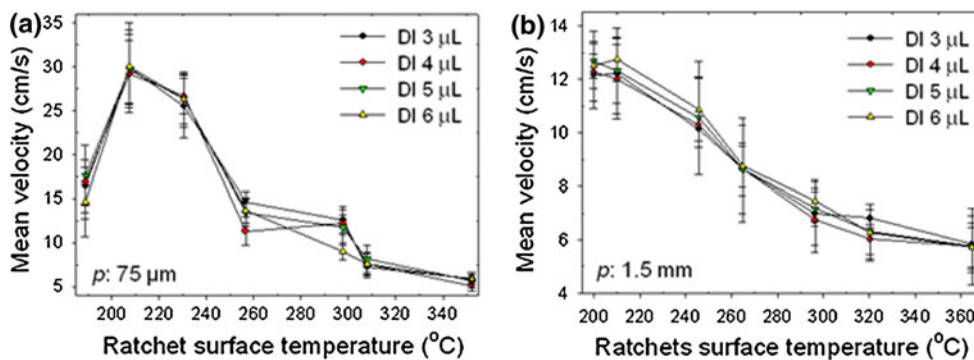
proportional to  $R^{4/3}$  (Biance et al. 2003; Linke et al. 2006). Another factor is that the droplet volume should be large enough, so that the droplet bottom covers at least one entire ratchet in order to induce unidirectional motion. This condition is met because the diameter for the smallest droplet volume used ( $2 \times 0.89$  mm for 3  $\mu\text{l}$  volume) is still larger than the largest ratchet period of 1.5 mm. When the droplet diameter was comparable to or smaller than ratchet period, then droplets motion along the ratched groove was observed.

Figure 8 shows mean droplet velocities of DI water with different volumes (3–6  $\mu\text{l}$ ) as a function of surface temperature for brass ratchet samples with 75  $\mu\text{m}$  and 1.5 mm period. The mean droplet velocities show a similar behavior to that described in Sect. 3.2. As the surface temperature increases, the increased vapor layer thickness underneath a droplet relative to the dimensions of ratchets increases, reducing the vapor pressure gradient and heat transfer between the ratchet peak and the droplet bottom. The temperature corresponding to the maximum mean velocities is the temperature when the heat transfer between the ratchet peaks and the droplet bottom is maximum. Since the droplet is not fully levitating from the surface, this temperature is still lower than  $T_L$ . In all temperature regimes, the droplet volume has a negligible effect on the mean velocity within the accuracy of the measurement. Intuitively, one could think that the mean velocity should increase with the increase of droplet volume because of the increased effective number of ratchets

In the higher temperature regime where the droplet is fully levitating from the surface, the positive effect from the increased number of ratchets on droplet propulsion is cancelled by the negative effect of increasing vapor layer thickness above the ratchet peaks, showing no dependence on the ratchet period



**Fig. 8** Mean droplet velocity as a function of ratchet surface temperature for different droplet volumes for ratchet samples with **a** 75  $\mu\text{m}$  period and **b** 1.5 mm period



within the effective length. However, this accelerating factor of increased effective number of ratchets with larger droplet volume seems to be cancelled out by the increase in the mass of the droplet to levitate and the increase in the vapor layer thickness (Biance et al. 2003).

### 3.4 Effect of surface energy of ratchet surface

We also investigated the influence of a hydrophobic silane coating on the ratchet surface on the droplet motion. Significant increase in hydrophobicity on the ratchet surface was achieved after the coating with almost uniform increase of the room temperature contact angles from  $(88\text{--}112) \pm 2^\circ$  to  $(111\text{--}128) \pm 2^\circ$  by  $\sim 20^\circ$  for all the ratchets. However, the actual contact mode at  $T_L$  regime may be determined by the contact angle at the boiling temperature. Figure 9 shows the mean droplet velocity as a function of ratchet surface temperature for ratchets with 800 nm and 1.5 mm period. The hydrophobic coating of the ratchet surface significantly affects the droplet motion in the L temperature regime, decreasing  $T_{Th}$  and increasing the maximum velocity. The result is in contrast to a theoretical study by Prat et al. (1995) for fully levitating droplets, where the round-off of the droplet due to surface tension does not seriously affect the flow field of the vapor. This in turn corroborates with our explanation for the droplet behavior in the L regime stating that there are local contacts between the peaks of the ratchets and the bottom of the droplet. In the presence of the direct contacts, a hydrophobic coating of ratchet surfaces seems to reduce the pinning force of droplets onto the ratcheted surface by reducing the contact area. The results indicate that  $T_{Th}$  can further be lowered by combining ratchets with superhydrophobic treatment chemically, topologically or the combination thereof.

## 4 Conclusions

We have shown the effect of ratchet period down to sub-micrometer on the motion of water droplets dispensed on

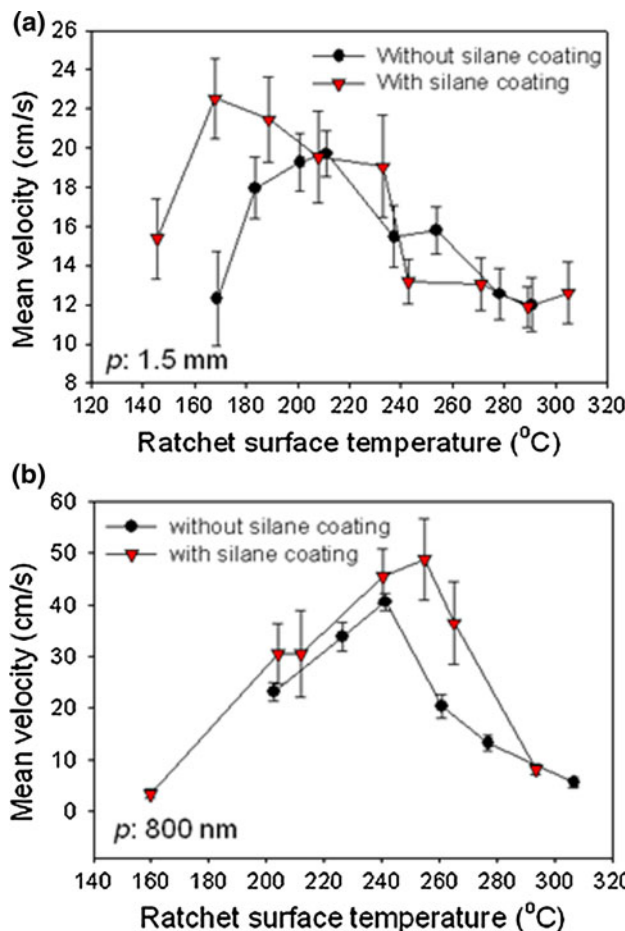


**Fig. 9** Mean droplet velocity as a function of ratchet surface temperature with and without a fluorinated silane coating **a** for brass 1.5 mm period and **b** Ni 800 nm period of ratchet surface

heated ratchet surfaces in the Leidenfrost regime. The maximum mean droplet velocity significantly increased as the ratchet period decreased, reaching  $\sim 40 \text{ cm/s}$  for sub-micron ratchets, which is attributed to the enhanced heat transfer through the ratchet peaks to the bottom of the droplet. The results suggest that even higher propulsion can be achieved with nanoscale ratchets and that micro- and nanoscale ratchets can potentially be used as a mechanism

to enhance film-boiling heat transfer associated with droplets and spray. Our results also show that driving levitating droplets using ratchets may be more effective in micro- and nanofluidic environments because droplets are usually squeezed by and thus touch the walls of micro- and nanochannels, enhancing the heat transfer between the droplet and the ratchets. Thus, micro- and nanoscale ratchets have a potential to be used as a component for droplet-based micro- and nanofluidic devices. In order to be able to provide a design rule for ratchet dimensions leading to the maximum droplet velocity, further systematic studies with different ratchet aspect ratios need to be performed. An application with high operation temperature is envisioned in microscale heat pipes incorporated with nanoratchets as closed loop, two-phase cooling systems with no moving parts and no external power for micro-processors. Use of low boiling point materials such as R134 will allow room temperature operation for this cooling application. Broader applications with micro- and nanoratchets can also be envisioned as a means of increasing efficiencies for film-boiling heat transfer associated with droplets and spray. One critical, but common problem in film-boiling heat transfer systems is that the presence of droplets bounced from the surface hinders a continuous heat transfer between injected droplets and hot surface, which can be avoided by using micro- and nanoratcheted surfaces. Those applications include fuel injection for combustion technology, stream generation for energy conversion in nuclear power energy converters, cooling systems for nuclear reactors, and spray quenching of heat treatable alloys.

**Acknowledgments** This research was supported by the National Science Foundation CAREER Award (CMMI-0643455). We also thank staff from the Center for Advanced Microstructures and Devices (CAMD) at Louisiana State University for the help in using microfabrication facilities in their cleanroom.

## References

- Bernardin JD, Mudawar I (1999) The Leidenfrost point: experimental study and assessment of existing models. *J Heat Transf* 121:894–903
- Bernardin JD, Mudawar I (2002) A cavity activation and bubble growth model of the Leidenfrost point. *J Heat Transf* 124:864–874
- Biance AL, Clanet C, Quere D (2003) Leidenfrost drops. *Phys Fluids* 15:1632–1637
- Brochard F (1989) motions of droplets on solid-surfaces induced by chemical or thermal-gradients. *Langmuir* 5:432–438
- Brzoska JB, Brochardwyart F, Rondelez F (1993) Motions of droplets on hydrophobic model surfaces induced by thermal-gradients. *Langmuir* 9:2220–2224
- Buguin A, Talini L, Silberzan P (2002) Ratchet-like topological structures for the control of microdrops. *Appl Phys* 75:207–212
- Chaudhury MK, Whitesides GM (1992) How to make water run uphill. *Science* 256:1539–1541
- Daniel S, Chaudhury MK, Chen JC (2001) Past drop movements resulting from the phase change on a gradient surface. *Science* 291:633–636
- Darhuber AA, Valentino JP, Davis JM, Troian SM, Wagner S (2003) Microfluidic actuation by modulation of surface stresses. *Appl Phys Lett* 82:657–659
- Ding Z, Song W-B, Ziaie B (2007) Time-multiplexed droplet manipulation via vibrating ratcheted micro-channels. *IEEE MEMS '07*. Kobe, Japan
- Ding Z, Song W-B, Ziaie B (2009) Sequential droplet manipulation via vibrating ratcheted microchannels. *Sens Actuators B* 142:362–368
- Dos Santos DF, Ondarchu T (1995) Free-running droplets. *Phys Rev Lett* 75:2972–2975
- Hughes MP (2004) Numerical simulation of dielectrophoretic ratchet structures. *J Phys D* 37:1275–1280
- John K, Bar M, Thiele U (2005) Self-propelled running droplets on solid substrates driven by chemical reactions. *Eur Phys J* 18: 183–199
- Julicher F, Ajdari A, Prost J (1997) Modeling molecular motors. *Rev Mod Phys* 69:1269–1281
- Kim N, Murphy MC, Soper SA, Nikitopoulos DE (2008) Investigation of two-phase flow in rectangular micro-channels. *ASME FEDSM*, Jacksonville
- Kulic IM, Thaokar R, Schiessel H (2005) A DNA ring acting as a thermal ratchet. *J Phys* 17:S3965–S3978
- Linke H, Humphrey TE, Lofgren A, Sushkov AO, Newbury R, Taylor RP, Omling P (1999) Experimental tunneling ratchets. *Science* 286:2314–2317
- Linke H, Humphrey TE, Lindelof PE, Lofgren A, Newbury R, Omling P, Sushkov AO, Taylor RP, Xu H (2002) Quantum ratchets and quantum heat pumps. *Appl Phys* 75:237–246
- Linke H, Aleman BJ, Melling LD, Taormina MJ, Francis MJ, Dow-Hygelund CC, Narayanan V, Taylor RP, Stout A (2006) Self-propelled Leidenfrost droplets. *Phys Rev Lett* 96:154502
- Ornatskii AP (1965) Generalization of experimental data on flow friction in surface boiling. *J Appl Mech* 6:80–82
- Prat M, Schmitz P, Poulikakos D (1995) On the effect of surface roughness on the vapor flow under Leidenfrost-levitated droplets. *J Fluids Eng* 117:519–525
- Thiele U, John K, Bar M (2004) Dynamical model for chemically driven running droplets. *Phys Rev Lett* 93:166602